Asian Journal of Advances in Research

5(1): 913-920, 2022

ENHANCEMENT IN MECHANICAL STRENGTH OF SLOW-COOLED QUADRUPLE PEROVSKITE $CaCu_3Ti_4O_{12}$ BY MICROWAVE-ASSISTED HEATING, AND RAPID THERMAL COOLING PROCESS

POOJA Y. RAVAL [a*], SHREY K. MODI [b], DOLLY J. PAREKH [c], NIKETA P. JOSHI [c], URMILA M. MESHIYA [c] AND KUNAL B. MODI [c]

[a] Department of Physics, C. U. Shah University, Wadhwan City, Surendranagar 363030, India.
[b] Department of Environment Engineering, L. D. Engineering College, Ahmedabad 380015, India.
[c] Department of Physics, Saurashtra University, Rajkot 360005, India.

AUTHORS' CONTRIBUTIONS

This work was carried out in collaboration among all authors. All authors read and approved the final manuscript.

Received: 25 April 2022
Accepted: 30 June 2022
Published: 05 July 2022

Original Research Article

ABSTRACT

The results of microwave-assisted heating and quenching process-induced modifications in elastic properties and lattice energy of slow-cooled microcrystalline $CaCu_3Ti_4O_{12}$ quadruple perovskite are presented. The X-ray density and mean atomic weight-based semi-empirical method was used to calculate longitudinal wave velocity that was further used to compute Debye temperature, several elastic constants, shear wave, and average sound velocities. The magnitude of elastic constants for microwave-assisted and quenched samples was found to enhance compared to the slow-cooled sample. The lattice energy values for microcrystalline ceramics were found to be smaller when compared with the lattice energy values for monocrystalline counterparts computed from three distinct approaches. It was found that the thermal history-induced modifications in structural and microstructural parameters govern the mechanical strength of the material.

Keywords: Calcium-copper-titanate; mechanical properties; thermal history.

1. INTRODUCTION

Pristine and substituted calcium-copper-titanate ($CaCu_3Ti_4O_{12}$) in monocrystalline, microcrystalline, nanocrystalline, and thin-film forms prepared and characterized by several experimental techniques are subject of interest from the year 2000 [1,2]. Typical frequency and temperature-dependent dielectric performance and current density against electric field characteristics make them suitable for super-capacitor and low/ high voltage varistor applications respectively. Accordingly, scores of research reports delineate different physical properties available in the literature [3 and references therein].

An ultrasonic pulse transmission method is referred to as the customary non-destructive experimental tool for the elastic moduli and Debye temperature determination. This technique applies to a large class of materials like spinel ferrites, garnets, superconductors, manganite perovskites, quadruple perovskite, composites, etc. [4-12]. In the investigation of elastic properties of nanoparticulates, monocrystals, and treated materials, where a small

**Corresponding author: Email: pooja.raval21@gmail.com;*

amount of sample is available, such a technique may not be useful. In the case of cubic structured spinel ferrites and garnets, elastic parameters can be determined from the cation distribution, infrared spectral analysis [13], and Raman spectral analysis [14]. On the other hand, density functional theory is used to calculate various elastic parameters [15], which involves detailed knowledge of the structure and cumbersome calculations.

We have employed here, a very simple X-ray density-based semi-empirical method [16] to determine and investigate external stimuli engendered modifications in elastic properties of phase pure $CaCu_3Ti_4O_{12}$. Elastic modulus is an inherent property of material while hardness is an engineering property. From rudimentary research aspects, the comprehension of elastic constants of given multi-crystalline materials is of much significance since they explicate the nature of binding forces in solids and explain the thermal properties of the solids. When we anticipate the usage of given microcrystalline material, besides the understanding of its magnetic, electric, and dielectric parameters, the knowledge of elastic properties assists to plan the appropriateness of the material for discrete applications. One can expect the development of large stresses inside polycrystalline materials when they are under the influence of high pressure, high temperature, large magnetic field, or huge electric field. The mechanical strength, toughness of structure, and thermal shock resistance are represented by elastic moduli values. Thus, the mechanical properties play a vital role while incorporating the material into a functional device [13,17].

As far as we know, very few research reports [10,11,18] discussing elastic properties of $CaCu_3Ti_4O_{12}$-based systems are available in the literature. The dielectric and elastic properties of $MgTiO_3$ – doped $CaCu_3Ti_4O_{12}$ polycrystalline materials employing the pulse-echo overlap technique have been studied by Rajmi et al. [11]. It has been observed that the substitution of $MgTiO_3$ in $CaCu_3Ti_4O_{12}$ caused an increase in shear and longitudinal velocities and related elastic constants indicating an improvement in elastic properties. Elastic modulus and hardness of pristine polycrystalline compositions, calcium titanate, calcium-copper-titanate, and its mixture have been investigated by Ramirez et al. [10]. It was found that $CaCu_3Ti_4O_{12}$ exhibited higher mechanical properties while $CaTiO_3/CaCu_3Ti_4O_{12}$ mixture showed intermediate properties between $CaTiO_3$ and $CaCu_3Ti_4O_{12}$. It is also concluded that $CaCu_3Ti_4O_{12}$ demonstrates excellent mechanical properties in contrast to other standard electroceramics. The effect of Na, Y, and Yb substitution on temperature-dependent elastic properties of single-crystalline $CaCu_3Ti_4O_{12}$ has been investigated by Yoshizawa et al. [18]. Elastic constants show an anomaly related to the antiferromagnetic transition at 24 K. In short, scarcely and limited information is available on the elastic behavior of $CaCu_3Ti_4O_{12}$. Besides, not a single report is available on the experimental or theoretical determination of lattice energy for $CaCu_3Ti_4O_{12}$-based systems in the literature. To explain the character, reactivity, stability, and structure of solid materials, lattice potential energy is mentioned as one of the paramount quantities. It is a very difficult task to experimentally determine the lattice energy by employing ancillary thermodynamic data from the Born-Haber-Fajans thermodynamic cycle, particularly for complex oxide systems. Consequently, alternate methods of lattice energy determination are of prime importance to researchers.

An interesting outcome of our previous investigations on consequences of thermal history (slow-cooling, rapid thermal cooling, and microwave-assisted heating) on electrical characteristics [19], magnetic ordering [20], positron annihilation lifetime parameters [21], and Raman spectral signature [22], prompted us and the dearth of elastic properties in treated $CaCu_3Ti_4O_{12}$ cubic perovskite in particular therefore motivates the present research. In this communication, the consequences of microwave-assisted heating, and quenching-induced modifications in elastic properties of slow-cooled polycrystalline $CaCu_3Ti_4O_{12}$ quadruple perovskite have been studied. The X-ray density-based semi-empirical method has been used to calculate longitudinal wave velocity that in turn is used to calculate shear velocity, mean sound velocity, various elastic moduli, Debye temperature, lattice energy, etc.

2. EXPERIMENTAL DETAILS

About 20 grams of a microcrystalline sample of $CaCu_3Ti_4O_{12}$ was prepared by the most widely used two-step solid-state chemical reaction route. An appropriate amount of high purity (≥ 99.5 %) metallic oxides, calcium carbonate, cupric oxide, and titanium dioxide, were thoroughly ground in an agate mortar and pestle, pelletized, and pre-sintered for 12 hours at a temperature of 1223 K, and then gradually cool down to room temperature (T = 300 K). In the final-sintering process, the re-grinded and re-pelletized sample was again held at T = 1423 K for 18 hours. Few pellets of the sample were slowly furnace cooled to 300 K by maintaining a cooling rate of 120 °C/hour (slow-cooled sample). On the other hand, a few pellets of the sample were rapidly cooled from the final sintering temperature (T = 1423 K) to liquid nitrogen (LN_2) temperature (T = 80 K) (ΔT = 1343 K)

(quenched sample). A set of the slow-cooled sample was heated further for 1 hour using a Kenstar make convection microwave oven (model OM 30 DCF) operating at a specific frequency of 2.45 GHz and having magnetron generated output microwave power of 900 watts (microwave-assisted sample).

The study on phase formation and structural parameters determination was carried out by analyzing X-ray powder diffraction (XRD) profiles registered with a Philips, Holland X-pert, automated multipurpose diffractometer using Copper Kα radiation with a wavelength of 0.154056 nm, graphite monochromator, and proportional counter filled with Xenon gas. The influence of thermal history on grain morphology of all three sets of the sample was investigated by scanning electron microscopy (model ESEM EDAX XL- 3D , Philips, Netherlands).

3. RESULTS AND DISCUSSION

The XRD profiles registered at T = 300 K for slow-cooled, microwave-assisted, and quenched samples of quadruple perovskite, $CaCu_3Ti_4O_{12}$, are depicted in Fig. 1. The refinement and indexing were accomplished by 'Powder –X' software [23]. The diffraction peaks can be indexed by the cubic body-centered perovskite-related structure, $CaCu_3Ti_4O_{12}$, following the Joint Committee on Powder Diffraction Standards (JCPDS) card # 75 – 2188 in which all planes are indexed.The analysis has confirmed that all the samples possess a monophasic cubic perovskite structure (space group *Im*3 No. 204 and point group T_h). No extra reflections analogous to any other crystallographic phase or un-reacted ingredients were traced out. The lattice constant (a) values thus determined are given in Table 1.

The X-ray density (ρ_x) of the samples was computed by adopting the formula stated by Smith and Wijn [24]:

$$\rho_x = \frac{ZM_w}{N_A a^3} \quad (1)$$

where M_w is the molecular mass of the composition (614.33 g/mol), N_A the Avogadro´s number. As there is 2 formula unit in the unit cell, Z=2 is taken in the formula. The structural parameters such as unit cell volume (V), ρ_x, bulk density (ρ), and pore fraction (f = 1 - (ρ/ρ_x)) for all the three samples are as well comprised in Table 1 to ease the further calculations, analysis, and discussion.

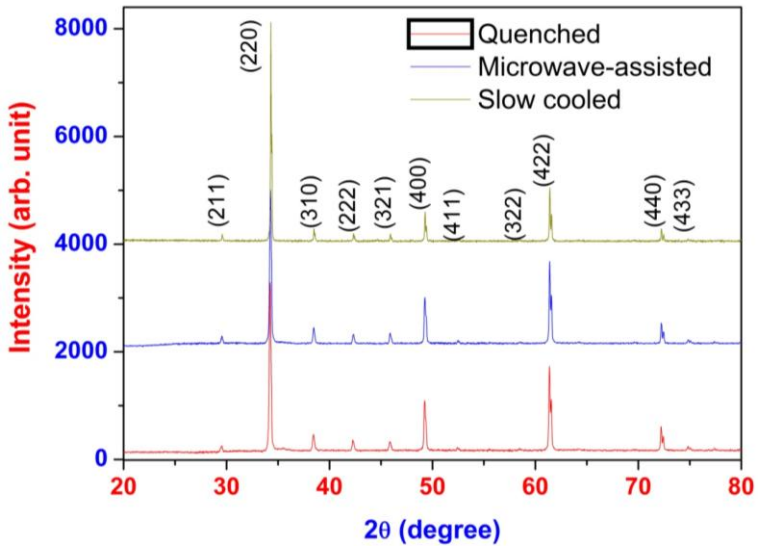

fig. 1. XRD profiles for differently treated samples of $CaCu_3Ti_4O_{12}$

Table 1. Structural, microstructural parameters and elastic wave velocity (V) for treated samples of $CaCu_3Ti_4O_{12}$ at 300 K

Sample	a(Å)	V(Å^3)	ρ_x ρ (g/cm^3)		f	D (μm)	V_{l0} V_{s0} V_{m0} (m/s)		
Slow-cooled	7.3925 (5)	403.98 (4)	5.052	4.590	0.0914	3.7	8062.1	4654.5	5167.7
Microwave-assisted	7.3810 (2)	402.12 (2)	5.075	4.070	0.1981	2.5	8138.3	4698.3	5216.5
Quenched	7.3785 (2)	401.71 (2)	5.081	4.468	0.1206	3.2	8158.1	4709.9	5229.2

Fig. 2 portrays scanning electron photomicrographs (SEM) captured from the fracture surface of highly compact pelletized samples. It is viewed that the morphology of grains (shape, size, distribution of grains, etc.) is extremely influenced by the employed heat treatment. The mean grain size has been estimated with the help of public domain software 'Image *J*'. It is observed that for the slow-cooled sample, grains are stuck to one another in a systematic manner that forms a reticular structure. The perceived transgranular fracture mode signifies that grain boundaries are of higher or equivalent strength than that of grains [25]. The mean grain size is found to be 3.7 μm. Scanning electron micrograph of microwave-assisted sample displays diffused grain structure along with a large number of pores. Thus, one can expect a lowering in bulk density and large pores fraction values as compared to slow-cooled and quenched samples (Table 1). It is found that the aggregate grain size is 2.5 μm. The quenched sample of $CaCu_3Ti_4O_{12}$ possesses a clearly defined grain structure. The grains are of pebble shape. The rapid thermal cooling process is responsible for this intragranular fracture mode [26]. The formation of a smooth bumpy surface where grains can be identified with ease is owing to the growth and transmission of this fracture along the grain boundaries. The aggregate size of grains is estimated to be 3.2 μm. It is fascinating to notice that with the quenching process, homogeneity, and uniformity of grains improve as well as void density is found to increase. During the synthesis process, the formation of voids cannot be prevented and that is restricted to the grains. These voids have distinct forms and dimensions not only but their distribution is also different that in turn affects the various physical properties. The grain morphology of slow-cooled, microwave-assisted, and quenched samples of $CaCu_3Ti_4O_{12}$ are accordant with the reported one [25-28].

In the instance of a wide range of silicates and oxides that include chromites, aluminates, spinels, ferrites, and garnets owning the alike mean atomic weight (*m*), the velocity of longitudinal waves (V_{l0}) is directly proportional to the ρ_x [16]. In the present investigation, all the three treated samples of $CaCu_3Ti_4O_{12}$ possess the same molar mass (M_w) and thus have the same value of $m = M_w/q = 33.717$ g/mol, (where *q* is the total number of atoms in the molecule (q = 20 for $CaCu_3Ti_4O_{12}$). Following the work, the V_{l0} (km/s) in terms of ρ_x (g/cm^3) and a(*m*) (km/s), the function of *m* is given by :

$$V_{l0} = a(m) + 3.31.\ \rho_x \qquad (2)$$

In the act of approximating the a(*m*) value for astated value of *m* we have contemplated the values of *m* and corresponding values of a(*m*), (for *m* = 21, a(*m*) = (-2.55) km/s, for *m* = 25, a(*m*) = (-5.7) km/s, and for *m* = 30, a(*m*) = (-8.6) km/s) [16]. For the multicationic oxide composition, $CaCu_3Ti_4O_{12}$, with *m* = 33.717 g/mol, the function a(*m*) is estimated to be (-8.66) km/s applicable to all three sets of the sample. The calculated values of V_{l0} and ρ_x are in turn used to deduce other elastic parameters, shear or transverse wave velocity (V_{s0}), mean sound velocity(V_{m0}), modulus L_0, G_0, B_0, E_0, σ_0, Lame´s constant (λ_{L0}), Vickers micro-hardness (H_{v0}) and characteristic Debye temperature (θ_0) in a void-free state using following standard formulae [4,12]:

$$V_{s0} = \frac{V_{l0}}{\sqrt{3}}$$

$$V_{m0} = \left[\frac{(3\,V_{l0}^3 \cdot V_{s0}^3)}{(2\,V_{l0}^3 + V_{s0}^3)}\right]^{1/3}$$

longitudinal modulus, $L_0 = \rho_x V_{l0}^2$

rigidity modulus, $G_0 = \rho_x V_{s0}^2$

bulk modulus $B_0 = L_0 - \frac{4}{3} G_0$

Poisson ratio, $\sigma_0 = \frac{(3B_0 - 2G_0)}{(6B_0 + 2G_0)}$

Young´s modulus, $E_0 = 2\,(1 + \sigma_0)\,G_0$

$$\lambda_{L0} = L_0 - 2\,G_0$$

$$H_{v0} = \frac{[(1-2\sigma_0)]\,E_0}{6\,(1+\sigma_0)}$$

and,

$$\theta_0 = \left(\frac{h}{k}\right)\left[\frac{(3\,N_A)q\,\rho_x}{4\,\pi\,M_w}\right]^{1/3} V_{m0} \qquad (3)$$

Where h is Planck´s constant and k is Boltzmann´s constant.

The calculated values of elastic parameters are summed-up in Tables 1 and 2. In the literature, no reported values of such parameters, except E_0 = 256 GPa and the upper limiting value of H_{v0} = 14.2 GPa determined from Hysitron Triboindenter by Ramirez et al. [10] are available for the comparison purpose. The value of σ_o for a stable, isotropic, and linear elastic material is larger than (-1) and lower than 0.5 owing to the need for E_0, G_0, and B_0 to have positive values. The σ_o is found to be ~ 0.25 for the different samples (Table 2), following the isotropic elasticity theory. Besides, data analysis turnout the following equation for the dependence of σ_o as a function of pore fraction (*f*) given by $\sigma_o(f) = 0.324\,(1\text{-}1.043\,f)$ [4]. The calculated values σ_o are found in the range of 0.26 - 0.29 for the studied samples in conformity with the calculated values from elastic moduli (Table 2). Young´s modulus, among all the elastic moduli, is of

particular attentiveness since it is the key parameter for the most frequently used core shapes viz. rings and rods [13]. The parameter, λ_{Lo}, has no physical explication, yet it assists in sampling the stiffness matrix in Hooke´s law. To understand solid-state problems that involve lattice vibrations, such as electrical resistivity, scattering of the thermal neutron, and thermal conductivity, θ_0 is a salient parameter. The temperature at which maximum vibrations occur is known as θ_0. The θ_0 value is found to increase for microwave-assisted and quenched samples as against the slow-cooled sample, suggesting that the lattice vibrations are hindered, which enhances elastic wave velocity and magnitude of elastic moduli as noticed.

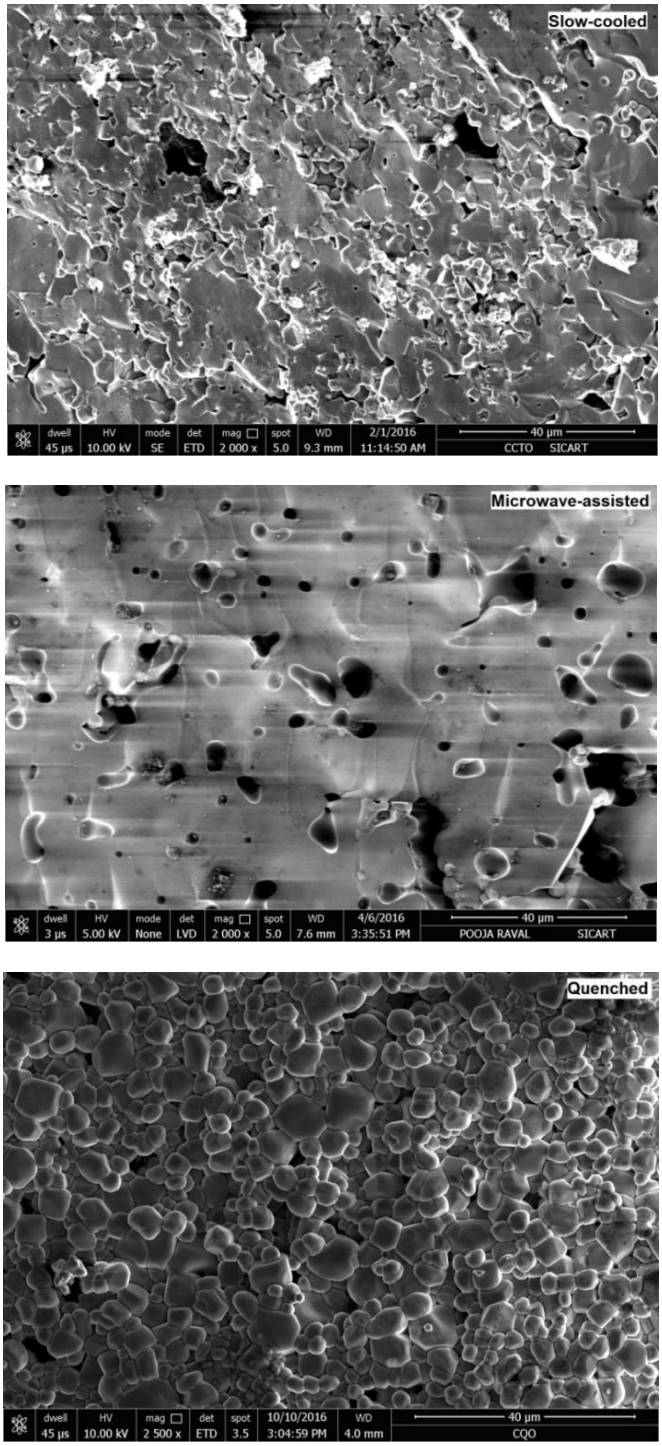

Fig. 2. SEM of differently treated samples of $CaCu_3Ti_4O_{12}$

Table 2. Elastic moduli for cubic perovskite, $CaCu_3Ti_4O_{12}$

Sample	L_0	G_0	B_0	E_0	λ_{L0}	H_{V0}	σ_0	θ_0 (K)
				(GP_a)				
Slow-cooled	328.36	109.05	182.43	273.13	109.44	18.24	0.25	711.83
Microwave- assisted	336.10	112.02	184.74	280.05	112.06	18.67	0.25	719.65
Quenched	338.16	112.71	187.88	281.78	112.74	18.79	0.25	720.12

Notably, the magnitude of elastic constants increases when a material is subject to microwave-assisted heating and quenching process. This enhancement in the mechanical strength of the material can be explained as follows. In the standard heating process, the material is heated from the surface to the inner core (i.e., temperature gradient) giving rise to thermal stress, and for the homogenization, a prolonged time is needed. In the microwave-assisted heating process, heat transfer is unvarying throughout the surface being volumetric heating in which microwaves interact with the material at the molecular level. This uniform temperature distribution all over the material maximizes the physical and mechanical properties. The rate of cooling of a specimen is decided by the rate at which the heat energy extraction takes place that further relies on the characteristic of the quenching medium in contact with the surface of the specimen besides the dimension and shape of the specimen. The mechanical strength of inorganic polycrystalline materials may be intensified by deliberately persuading compressive residual surface stresses. The technique of heat treatment called quenching can execute this. In this process, the material is heated to an elevated temperature, sustained for a few hours, and is then cooled to ambient temperature in a disparate quenching media. In this investigation pelletized $CaCu_3Ti_4O_{12}$ polycrystalline composition was heated to 1323 K, kept for 18 hours and it is then cooled to room temperature employing liquid nitrogen (T = 80 K) as a quenching medium. The residual stresses ensue from dissimilarity in the rate of cooling of the interior region and surface region. At first, the surface cools down quickly and, once trapped to a temperature lower than the strain point, set off rigid. At this juncture, the inner region, having cooled slowly is at a higher temperature (exceeding the strain point). On continuing cooling, the interior region seeks to shrink to a higher extent as compared to what the new rigid outer region will permit. Consequently, the inside tends to draw on the outside or impose inward radial stresses. Thus, after the material cools- down to ambient temperature, it undergoes compressive stresses on the surface, with tensile stresses in the interior region; subsequently, the magnitude of elastic constants increases. The perceived improvement in elastic strength of microwave-assisted and quenched cubic perovskites as compared to the slow-cooled counterpart (Table 2) may be due to the change in interionic distances. It is seen from Table 1 that a (Å) decreases for the microwave-assisted sample (Δa = 0.0115 Å) and quenched sample (Δa = 0.0140 Å) as against the slow-cooled sample. Subsequently, interionic distances are expected to lessen. This strengthens the bonding, thus the magnitude of elastic moduli is anticipated to enhance as observed.

The reduction in grain size, 3.7 μm for a slow-cooled sample to 3.2 μm for a quenched sample to 2.5 μm for a microwave-assisted sample, can not be the governing factor for observed enhancement in the mechanical strength of the microwave-assisted and quenched samples at least in micron-size grains. Besides grain size, the elastic constants are significantly affected by the presence of a secondary phase, impurities, geometry, and distribution of pores. But improvision in microstructure has a positive effect on mechanical strength. The partial removal of internal micro-cracks by the rapid thermal cooling process may also be responsible for observed strengthening.

The values of B_o and G_o are further used to calculate Pough´s ratio (B_o/G_o) and Frantesvich´s ratio (G_o/B_o). Accordingly, if B_o/G_o is less than 1.75 and G_o/B_o is greater than 0.571, the material becomes brittle while if B_o/G_o is greater than 1.75 and G_o/B_o is less than 0.571, the material becomes ductile. On the other hand, if Poisson´s ratio is higher than 0.33, the material possesses ductile nature while it is brittle with $\sigma_o < 0.33$ [15]. In the present case, B_o/G_o is found to be ≈ 1.67, G_o/B_o is found to be ≈ 0.6, and $\sigma_o \approx 0.25$ for the different samples of $CaCu_3Ti_4O_{12}$. The calculated values of ratios lead to conclude that the samples exhibit brittle nature under ambient conditions.

"The elastic moduli and their pressure derivatives are suggestive of the short-range contributions to the lattice energy. Consequently, the parameters influencing the value of elastic moduli are further concomitantly accountable for controlling the lattice energy (strength of bonding) (U_L). In ionic solids, the strength of bonds present can be estimated from the calculation of U_L. The U_L of such ionic compounds can be calculated from the most conventional Kudriavtsev´s approach" [29]. With certain

assumptions, well discussed in [5,13,14], this can be further simplified and used to calculate lattice energy for micro-crystalline materials (U_{LP}). The resultant equation is given by :

$$U_{LP}\,(eV) = (-\,3.108 \times 10^{-5})\,(M_w\,(kg/mol) \times V_{m0}\,(m/s)) \quad (4)$$

The calculated values of U_{LP} for all three samples are summed- up in Table 3.

Table 3. U_L Lattice energy for treated samples of polycrystalline $CaCu_3Ti_4O_{12}$ composition

Sample	$-U_{Lp}$ (eV)	$-U_{Ls}$ (eV)
Slow-cooled	509.9	683.98
Microwave-assisted	519.6	685.02
Quenched	522.1	685.29

The lattice energy determination for single crystals by Kapustinskii´s approach [30] is found quite outstanding to compute U_L for a great variety of monocrystalline materials (U_{LS}). Accordingly,

$$U_{LS}\ (kJ/mol) = \left[\frac{(-1202.5 \times q \times |Z^+||Z^-|)}{(r^+ + r^-)}\right] \times \left[1 - \frac{(0.345)}{(r^+ + r^-)}\right] \quad (5)$$

Here, Z^+ is the weighted mean of cationic charge, Z^- is the mean ionic charge of the anion (i.e., oxygen), r^+ is the weighted mean ionic radius of metallic cations involved (0.701 Å) and r^- is the ionic radius of oxygen (1.32 Å). The U_{LS} is found to be (- 606.93 eV) applicable to slow-cooled, microwave-assisted, and quenched samples.

"The lattice potential energy of complex ionic solids has also been determined employing the limiting relation between U_{LS}, M_w, and ρ_x suggested" by Glasser and Jenkins [31] :

$$U_{LS}\,(kJ/mol) = \left(\frac{(\rho_x \times N_A \times 2I^4 \times A^3)}{10^{21} \times M_w}\right) \quad (6)$$

where *A* is the standard electrostatic conversion term equal to 121.39 kJ/mol/nm, *I* (= 64) is the ionic strength-related term. The factor 10^{21} converts cubic nanometer to cubic meter. In Table 3 the calculated values of U_{LS} are presented in eV for the comparison purpose for the three sets of $CaCu_3Ti_4O_{12}$ composition.

To compute the lattice energy of $CaCu_3Ti_4O_{12}$ oxide composition we have to diversify the relevancy of the oxide additivity rule employed to approximate the dielectric and electronic polarizability for complex oxide compositions [32], by taking into consideration the lattice energy of constituent oxides [33], CaO, CuO and TiO_2 (U_{LS} (CaO) = -3401 kJ/mol, U_{LS} (CuO) = -4050 kJ/mol and U_{LS} (TiO_2)) = -12054 kJ/mol). Accordingly,

$$U_{LS}\ (CaCu_3Ti_4O_{12}) = [(1)\ U_{LS}\ (CaO) + (3)\ U_{LS}\ (CuO) + (4)\ U_{LS}\ (TiO_2)] \quad (7)$$

"The computed lattice energy value is found to be (-63767 kJ/mol) = (-653.61 eV). This value is in good accord with that computed using other models and validate the present approach. This methodology was successfully employed earlier for lattice energy determination for many spinel ferrites, garnets, and superconducting oxide systems" [34] and may be extended to other complex oxide systems also.

"It is found that the lattice energy values (U_{LP}) for polycrystalline treated samples of $CaCu_3Ti_4O_{12}$ composition are much lower than their monocrystalline counterparts (U_{LS}) calculated using three different approaches. The observed difference between the two (U_{LP} U_{LS} and $U_{LS} > U_{LP}$) can be manifested in this way. Microcrystalline materials possess several small crystals or grains. The neighboring grains with distinct crystallographic orientations are separated by a grain boundary, which is a certain atomic distance wide region. It is possible to have varying degrees of crystallographic misalignment among adjoining grains. The atoms along a grain boundary are less regularly bounded as bond angles are large and that results in grain boundary energy. The degree of disorientation decides the magnitude of grain boundary energy, being larger for high angle boundaries" [35,36]. These grain boundaries prevent the long-range range interactions. The lattice energy value for microcrystalline materials is lower than that of monocrystalline materials, and this is the most likely reason (Table 3).

4. CONCLUSION

It is inferred that the X-ray density and mean atomic weight-based semi-empirical method is simple and successful for various elastic parameters determination. The observed improvement in mechanical strength of quenched and microwave-assisted samples as against a slow-cooled sample of polycrystalline $CaCu_3Ti_4O_{12}$ ceramic is owing to the compressive surface stresses and tensile stresses at interior regions induced in the material as well as constructive modifications in structural and microstructural characteristics. The magnitude of Pugh, Frantesvich, and Poisson ratios suggests that the cubic perovskites are brittle. The lattice potential energy values for microcrystalline materials are found to be smaller as compared to monocrystalline counterparts mainly caused by the role played by grain and grain boundary to multi-crystalline materials. The elastic properties and lattice energy are highly affected by the heat treatment employed.

COMPETING INTERESTS

Authors have declared that no competing interests exist.

REFERENCES

1. Subramanian MA, Li D, Duan N, Reisner BA, Sleight AW. J. Solid State Chem. 2000; 151:323-325.
2. Ramirez MA, Subramanian MA, Gardel M, Blumberg G, Li D, Vogt T, Shapiro SM. Solid State Commu. 2000;115:217-220.
3. Jani KK, Barad DV, Raval PY, Nehra M, Vasoya NH, Jakhar N, ModiSandeep Kumar KB, Lim DK, Singhal RK. Ceram. Int. 2021;47:5542-5548.
4. Baldev R, Rajendran V, Palanichamy P. Science and technology of ultrasonics, (Norosa Publishing House, New Deli). 2004;78-81.
5. Lakhani VK, Modi KB. Solid State Sci. 2010;12(12):2134-2143.
6. Sharma PU, Modi KB. Phys. Scr. 2010; 81:015601(9).
7. Solunke MB, Sharma PU, Pandya MP, Lakhani VK, Modi KB, Reddy PV, Shah SS. Pramana – J. Phys. 2005;65(3):481–490.
8. Solunke MB, Sharma PU, Lakhani VK, Pandya MP, Modi KB, Reddy PV, Shah SS. Ceram. Int. 2007;33(1):21-26.
9. Buch JJU, Lalitha G, Pathak TK, Vasoya NH, Lakhani VK, Reddy PV. Ravi Kumar, Modi KB. J. Phys. D: Appl. Phys. 2008;41: 025406(10).
10. Ramirez MA, Parra R, Reboredo MM, Varela JA, Castro MS, Ramajo L. Mater. Lett. 2010; 64:1226-1228.
11. Rajmi R, Yahya AK, Yusof MIM. Aust. J. Basic Appl. Sci. 2011;5(8):405-416.
12. Malaeb W, Basma H, Me M, Barakat, Awad R. Supercond J. Nov. Magn. 2017;30:3595–3602.
13. Modi KB, Shah SJ, Pujara NB, Pathak TK, Vasoya NH, Jhala IG. J. Mol. Struc. 2013; 1049:250–262.
14. Modi KB, Raval PY, Shah SJ, Kathad CR, Dulera SV, Popat MV, et al. Chem. 2015; 54(4):1543 -1555.
15. Tariq S, Ahmed A, Saad S, Tariq S. AIP Adv. 2015;5:077111-1-9.
16. Birch F. Geo Phys. J. Int. 1961;4(Supp.-1):295–31.
17. Pathak TK, Buch JJU, Trivedi UN, Joshi HH, Modi KB. J. Nanosci. Nanotech. 2008; 8(8):4181-4187.
18. Ismayil A, Nakamura T, Kamiya R, Nakamura M, Nakanishi Y, Naito T, Fujishiro H, Watanabe T, et al. J. Phys. Soc. Jpn. 2011; 80:SA113 - 1-3.
19. Raval PY, Makadiya AR, Pansara PR, Sharma PU, Vasoya NH, JBhalodia A, et al, Mater. Chem. Phys. 2018;212:343-350.
20. Raval PY, Pansara PR, Makadiya AR, Vasoya NH, Dolia SN, Modi KB. Ceram. Int. 2018;44(15):17667-17674.
21. Meshiya UM, Jani KK, Mange PL, Barad DV, Raval PY, Modi KB, Nambissan PMG. Spect. Lett. 2019;52 (10):633-641.
22. Meshiya UM, Raval PY, Joshi NP, Vasoya NH, Upadhyay D, Jha PK, Modi KB, Vib. Spec. 2020;112(103201):10.
23. Dong C. Powder X: Windows -95-based program for powder X-ray diffraction data processing, J. Appl. Cryst. 1999;32(4):838 - 838.
24. Smith J, Wijn HPJ. Ferrites, (John Wiley and Sons, NY). 1959;5-21.
25. Huang Y, Shi D, Li Y, Li G, Wang Q, Liu L, Fang L. J. Mater. Sci. Mater. Electron. 2013;24(6):1994-1999.
26. Kumar R, Zulfequar M, Sharma L, Singh VN, Sanguttavan TD. Cryst. Growth Design. 2015;15(3):1374 -1379.
27. Yu H, Liu H, Luo D, Cao M. J. Mater. Process. Technol. 2008;208(1-3):145 -148.
28. Hutagalung SD, Ikhwan M, Ibrahim M, Ahmad ZA. Ceram. Int. 2008;34(4):939 -942.
29. Kudriavtsev BB,.Soviet. Phys. Acoust. 1956;2:172 -177.
30. Kapustinskii AF. Quart. Rev. Chem. Soc. 1956; 10:283-294.
31. Glasser L, Jenkins HDB. J. Am. Chem. Soc. 2000;122(4):632–638.
32. Shannon RD, Rossman GR. Am. Min. 1992; 77(1-2):94-100.
33. Mu L, Feng C, He H. MATCH Commun. Math. Comput. Chem. 2006;56:97-111.
34. Modi KB. J. Supercond. Nov. Mag. 2016; 29(9):2287- 2297.
35. Callister WD. Materials Science and Engineering: An Introduction, (John Wiley and Sons, NY); 2000.
36. Lila DL, Modi SK, Joshi NP, Raval PY, Vasoya NH, Modi KB, Joshi HH. Study on elastic, thermodynamic, and optical properties of $Y_2Ti_2O_7$ pyrochlore determined by a semi-empirical method at 300 K. Asian Journal of Advances in Research. 2021 Dec 6;219-30.